Silver Modified TiO₂/Halloysite Thin Films for Decontamination of Target Pollutants

Dionisios Panagiotaras, Elias Stathatos, Dimitrios Papoulis

Abstract—Sol-gel method has been used to fabricate nanocomposite films on glass substrates composed halloysite clay mineral and nanocrystalline TiO₂. The methodology for the synthesis involves a simple chemistry method utilized nonionic surfactant molecule as pore directing agent along with the acetic acid-based sol-gel route with the absence of water molecules. The thermal treatment of composite films at 450°C ensures elimination of organic material and lead to the formation of TiO₂ nanoparticles onto the surface of the halloysite nanotubes. Microscopy techniques and porosimetry methods used in order to delineate the structural characteristics of the materials. The nanocomposite films produced have no cracks and active anatase crystal phase with small crystallite size were deposited on halloysite nanotubes. The photocatalytic properties for the new materials were examined for the decomposition of the Basic Blue 41 azo dye in solution. These, nanotechnology based composite films show high efficiency for dye's discoloration in spite of different halloysite quantities and small amount of halloysite/TiO₂ catalyst immobilized onto glass substrates. Moreover, we examined the modification of the halloysite/TiO₂ films with silver particles in order to improve the photocatalytic properties of the films. Indeed, the presence of silver nanoparticles enhances the discoloration rate of the Basic Blue 41 compared to the efficiencies obtained for unmodified films.

Keywords—Clay mineral, nanotubular Halloysite, Photocatalysis, Titanium Dioxide, Silver modification.

I. INTRODUCTION

ONE of the main environmental problems which receives special attention in industry is the wastewater treatment. Textile colored effluents, paper pulp and other related industries have influenced the quality of the natural environment because of the wastewater disposal. Azo dyes used in the textile industry are resistant water pollutants provoke toxic effects in the aquatic systems. Azo dyes exhibit low degradation rates in the existing environmental conditions to the ultraviolet and solar light irradiation and also to biological treatment defied the development of innovative treatment technologies [1], [2]. These methods, called Advanced Oxidation Technologies (AOTs) have also used to the decontamination of polluted water. AOTs have a high efficiency to remove azo dyes from water based on the oxidative power of radical species created during these

Dionisios Panagiotaras is with the Mechanical Engineering Department, Technological-Educational Institute of Western Greece, 26334 Patras, Greece.

Dimitrios Papoulis is with the Geology Department, University of Patras, 26504 Patras, Greece.

Elias Stathatos is with the Electrical Engineering Department, Technological-Educational Institute of Western Greece, 26334 Patras, Greece (corresponding author to provide phone: 0030-2610-369242; e-mail: estathatos@teipat.gr).

processes. In addition photocatalysis one of the AOTs methods can be successfully applied to the oxidation and final removal of azo dyes with the formation of carbon dioxide as a final product. A variety of wide band gap semiconductors under UV or solar light have been used for the photocatalytic decomposition of various organic pollutants [3], [4]. Among them, TiO₂ is a high efficient material for the photo-degradation of many organic pollutants, while it is relatively inexpensive, non-toxicity and stabile in aquatic environments [5], [6]. Moreover, the mesoporous nanocrystalline anatase TiO₂ particles, films or membranes have extended uses in environmental remediation techniques [7]. The photocatalytic potency of the ultrafine TiO₂ powders is due to the high particle surface area since reactions take place on the surface of the nanocatalyst, but the agglomeration of the ultrafine TiO₂particles to larger aggregates decay the efficiency of the photocatalyst.

Nevertheless, although TiO₂ used as mobilized catalyst for its high catalytic surface area and activity [8], TiO₂ powders cannot easily be recovered from solutions when they are used for water purification. Highly dispersed ultrafine TiO₂ particles in suspension are difficult to recover from solution during water and wastewater treatment. To overcome this limitation, many researchers immobilize TiO₂ catalyst onto substrates as thin films and membranes. This technique, although lower the catalytic surface area compared to powder, extent the use and application of the photocatalyst because of the easy way to handle these materials in a variety of environmental applications [9]-[11]. A number of factors controlling the photocatalytic activity of the films such as the number of -OH surface groups, the specific surface area, particle morphology, possible aggregation and phase composition. However, modifications on the porous structure of this class of materials increase the photocatalytic properties of the catalysts. Activated carbon, glass slides and fibers, membranes, and zeolites are used among other sustainers in order to enhance the photocatalytic activity of the nanocomposites [12]-[14]. Degrease of the photocatalyst efficiency is due to the lower total surface area and the immobilization of the catalyst compare to the ultrafine pure TiO₂ powder. Nevertheless, much research has been done to overcome this limitation by using highly porous materials such as clay minerals as substrates for TiO₂particles immobilization [15], [16]. The clay mineral halloysite with tubular structure has been considered as a cheap and appropriate material used for TiO₂ particles immobilization [17], [18]. Additionally, many studies have been devoted to the improvement of titania photoactivity by depositing noble

metals. In particular, deposition of silver on TiO_2 colloidal particles has received an extended interest that goes beyond photocatalytic degradation. Thus metallic silver can be photocatalytically deposited on TiO_2 and this process can be used in silver recovery e.g. from waste photographic effluents.

In this work we use the sol-gel method with surfactant molecules in order to produce thin mesoporous nanocrystalline TiO_2 films in the presence of clay mineral halloysite nanotubes. We examined the efficiency of the new photocatalyst for the degradation of the azo-dye Basic Blue 41. Furthermore, the as-prepared nanocomposite thin films were modified with silver in order to enhance their photocatalytic efficiency. The silver modification of halloysite/TiO_2 nanocomposite photocatalysts immobilized on glass substrates is a promising technique for the degradation of azo dyes in solution and can be use for the water and wastewater treatment.

II. MATERIALS AND METHODOLOGY

A. Chemical Reagents

Pure and well crystalline halloysite samples with tubular morphology were originated from Utah, USA and they were size fractionated by gravity sedimentation to obtain sizes less than 2 μm. Separation of the clay fraction was carried out by using centrifugation methods. The clay fractions of the most halloysite-rich samples were used for the preparation of TiO_2–halloysite nanocomposites. Commercially available Triton X-100 (X100, polyethylene glycol tert-octylphenyl ether), titanium tetraisopropoxide (TTIP), acetic acid (AcOH), Basic Blue 41 (BB-41), silver nitrate (>99%) and all solvents were purchased from Sigma-Aldrich. Double distilled water with resistivity 18.2 MΩ (Millipore) was used in all experiments.

B. Sol-Gel Synthesis of Composite Halloysite/TiO_2 Sol

The X100 as a nonionic long chain surfactant organic molecule was selected as a pore directing agent in a sol. Such amphiphilic molecules may succeed the existence of ordered mesophase and the ability to adjust large inorganic clusters in aqueous condition at the same time. A suitable amount of X100 was homogeneously dissolved in ethanol. Before adding alkoxide precursor, AcOH was added into the solution for the esterification reaction with ethanol. Then, TiO_2 precursor, TTIP was added at a time under vigorous stirring. The molar ratio of the materials was optimized at X100: Ethanol: AcOH: TTIP = 1: 68: 6: 1 in accordance to previous published results [19]. Halloysite (HAL) powder was mixed with previous solution in various quantities following HAL 5%, 20%, 25% and 30% weight ratio compared to TiO_2 mass. After stirring for several minutes, the dispersion was ready to be used on glass slides. Films prepared on glass slides for the four HAL weight ratios will be referred as HT5, HT20, HT25 and HT30 respectively while HT0 represents pure TiO_2 films without the presence of halloysite.

C. Formation of TiO_2 Thin Films and Silver Modification

Borosilicate glass with a size of L75 mm (effective L60) × W25 mm × T1 mm was used as a substrate for fabricating immobilized HAL/TiO_2 thin films. Before coating, the substrate was thoroughly cleaned with detergent and washed with water and acetone and finally dried in a stream of nitrogen. A home-made dip-coating apparatus equipped with a speed controller to maintain a withdrawal rate of ~10 cm/min was used to dip in and pull out the substrate from the sol. After coating, the films were dried at room temperature for 1 hour, calcined in a multi-segment programmable furnace (PLF 110/30, Protherm) at a ramp rate of 5ºC/min to 450ºC for 15 min, and cooled down naturally. Only one layer of catalyst was formed for all HAL/TiO_2 ratios. In case that the as resulted films was chosen to be modified with silver, they were immersed in 1mM silver nitrate aqueous solution. The films were remained in the sol for 15 minutes and then they were rinsed with double distilled water and dried under nitrogen gas. Afterwards, they were exposed to black light (UV source) for 20 minutes while their color was turned to brown which means that adsorbed silver ions were reduced and they were converted to zero valence silver.

D. Instrumentation and Materials Characterization

Nitrogen intrusion/extrusion curves were measured with a Micromeritics Tristar 3000 and the surface area, porosity, and pore size distribution were derived by differentiating them according to BET method. The values were obtained from thick films after scratching the material due to the difficulty of sample collection from the thin films. A Bruker D8 Advance diffractometer with CuKα (λ = 1.5406 Å) radiation and Bragg-Brentano geometry was employed for X-ray diffraction (XRD) studies of the halloysite-TiO_2 catalyst. For the visual morphology of HAL/TiO_2 nanostructure, an environmental scanning electron microscope (FESEM, Zeiss SUPRA 35VP) was used and inspect film homogeneity. AFM images were obtained with a Nanoscope III, Digital Instruments, in the tapping mode. Absorption measurements of BB-41 sols were carried out with a Hitachi U-2900 UV-Vis spectrophotometer.

E. Photocatalytic Properties of Composite Films

For the photocatalytic experiments a cylindrical reactor was used which was presented in a previous publication [20]. Dry air was pumped through a gas inlet using a small pump to ensure continuous oxygen supply to the reaction solution while it was simultaneously agitated. Four Black lights with 4 W nominal power were placed around the reactor for UV illumination. The whole construction was covered with a cylindrical aluminum reflector. Cooling was achieved by air flow from below the reactor using a ventilator. The catalyst was in the form of four borosilicate glasses, covered on one side with nanocrystalline HAL%-TiO_2 films. The total surface of the photocatalyst films was approximately 60 cm^2. The reactor was filled with 75 ml of 2.5x10^{-5} M BB-41 aqueous solution. BB-41 is strongly adsorbed on pure or halloysite modified TiO_2 films. For this reason, we stored the solution in the presence of the photocatalyst in the dark for an hour and all of our photocatalytic results were obtained after equilibrium. The photocatalytic discoloration process for the dye was examined by monitoring the absorption maximum of

the BB-41 solution (λ=610 nm) at various irradiation times. Photocatalytic discoloration rate of BB-41 was calculated by the formula:

$$r = \frac{C_0 - C}{C_0} \qquad (1)$$

where C_0 is the initial concentration of BB-41 solution and C is the final concentration after irradiation with UV light. Discoloration efficiency was determined as:

$$efficiency\% = \frac{C_0 - C}{C_0} 100\% \qquad (2)$$

For the repeated use of the photocatalysts, the films were washed with double distilled water and dried at 80°C while no further treatment was followed for the films. The adsorption of BB-41 on HAL-TiO$_2$ films was examined under dark and after 1 hour presence of the films in dye's aqueous solution.

III. RESULTS AND DISCUSSION

A. Structural Characteristics of Halloysite and TiO$_2$ Nanocomposite Films

The composite Halloysite/TiO$_2$ films were prepared on borosilicate glass substrates for different HAL weight proportions as described in experimental section. Samples, abbreviated as HT5, HT20, HT25 and HT30 represent the different weight proportions of halloysite in TiO$_2$ sol while HT0 is referred to pure TiO$_2$ films. After calcination at relatively high temperature ≈450°C to eliminate organic substances all films were firmly attached on the glass without any cracks because of TiO$_2$content. Halloysite was finely dispersed in the films for any proportion was used. First, the crystallinity of the films was examined in order to detect any differences to the crystal structure of halloysite after heating and the crystal phase of resulting nanocomposite TiO$_2$. The XRD patterns of all films are presented in Fig. 1.
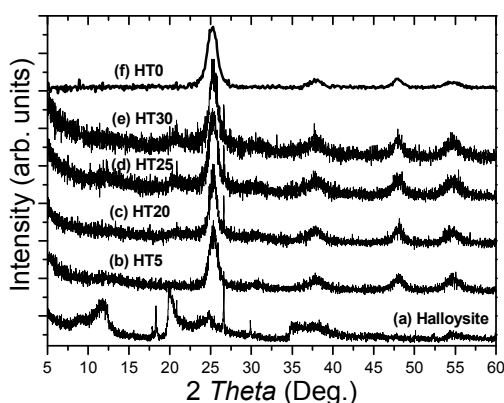

Fig. 1 XRD patterns of Halloysite-TiO$_2$ nanocrystalline films: (a) halloysite clay mineral (b) HT5, (c) HT20, (d) HT25, (e) HT30, (f) HT0.

Strong reflection at 2θ=12.2° is corresponded to halloysite 7Å, while a less intensive reflection at 2θ equal to 8.80° corresponds to halloysite 10Å (Fig. 1, curve a). The main peak of halloysite 7Å seems that is remaining after heating but it is much lower mainly to the low amount of the mineral in films proving the remaining crystallinity of the clay mineral. A second reason is probably the partial dehydration of halloysite due to the temperature applied for the synthesis of the films. It should be noted that in this sample (Fig. 1, curve a) low amounts of quartz are also present (main reflections observed at 26.60° and 20.80°).Titania pure nanocrystalline film (HT0) is also presented in Fig. 1 (curve f) where a reflection (101) of anatase form at 2θ=25.1° is observed. The two basic reflections at 2θ=12.2° and 2θ=25.1° for HAL and TiO$_2$ are maintained at the rest of samples with different intensity ratio because of the variable proportion between them. The grain size for TiO$_2$ has been calculated from XRD patterns using Scherrer's equation:

$$D = 0.9\lambda/(s\,cos\theta) \qquad (3)$$

where λ is the wavelength of the X-ray and s is the full width (radians) at half maximum (FWHM) of the signal. The crystallite size for TiO$_2$ is calculated 7.5, 8.1, 11.3, 8.5 and 9.4 nm for samples HT0, HT5, HT20, HT25 and HT30 respectively.

TABLE I
STRUCTURAL CHARACTERISTICS OF HALLOYSITE-TiO$_2$ FILMS

Sample	Total pore volume V_p (cm³/g)	Specific surface area S (m²/g)	Total porosity φ(%)	Mean pore diameter D_{por} (nm)
Halloysite	0.125	50.9	24.46	9.85
HT0	0.133	121.3	33.58	4.78
HT5	0.165	108.6	39.10	6.09
HT20	0.155	77.5	37.62	7.98
HT25	0.171	95.3	39.95	7.20
HT30	0.159	106.2	38.21	6.01

All the peaks indicated that the crystal phase of the materials containing TiO$_2$ was anatase and the relatively large width of peaks indicated that the size of the nanocrystallite was less than 12 nm. It should be noted that it is evident from the XRD patterns that the calcination at 450°C for 15 min did not damaged halloysite clay.

Because of the difficulty in directly characterizing the porosity of immobilized Halloysite/TiO$_2$ thin films, the characterizations were carried out on the corresponding particles. The specific surface area S, the total pore volume V_p, the mean pore diameter D_{por}, and the total porosity φ were calculated for all samples and they are presented in Table I.

Pure halloysite powder has relatively large pore volume and similar to that obtained for pure TiO$_2$ while their mixtures possess slightly greater values. As it concerns the particle surface areas, in the case of pureTiO$_2$ a relatively high value of 121.3 m²/g is measured and 50.9 m²/g for halloysite. All other samples with different proportions of halloysite in TiO$_2$ matrix appear intermediate values for particle surface areas as they appear in Table I.
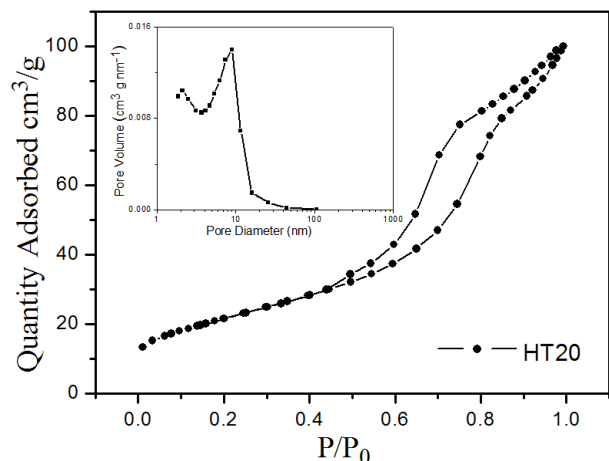
Fig. 2 Sorption-desorption isotherm and pore size distribution (inset) for HT20 thin film

Nitrogen sorption-desorption curves for all Halloysite/TiO$_2$ samples were obtained. However, as an example we present the data obtained for HT20films in Fig. 2, while pore size distribution appear as an inset of the same figure. This porosity is, also, apparent in SEM images shown in Fig. 3. Halloysite samples are consisted of tubular particles as it can be seen in Fig. 3 (a). TiO$_2$ –Halloysite modified are presented in Fig. 3 (b). The average diameter of the tubes, as they were observed before modification, is 40-70nm while the length is between 100-500nm. After modification, TiO$_2$ nanoparticles uniform in size overlay halloysite tubes.

Besides, TiO$_2$ nanoparticles help to the stabilization of the composite material on the borosilicate glass substrate after calcination by forming stable Ti-O-Si bonds [21], [22]. In Fig. 3 (b) halloysite nanotubes seem to be completely covered with uniform layers of TiO$_2$ and uniform particle distribution. The thickness of TiO$_2$ film without halloysite tubular particles is around 180-200 nm with only one dipping layer according to a cross sectional SEM image.

The homogeneity of TiO$_2$ particles' size and film can be also seen in Fig. 3 (b). According to the same image of Fig. 3 the TiO$_2$ crystal grains have a spherical shape while they have an average size ranging from 12 to 16 nm. TiO$_2$ particles were also found to form aggregates on halloysite external surfaces but these were of uniform small size as it was also proved by porosimetry data.
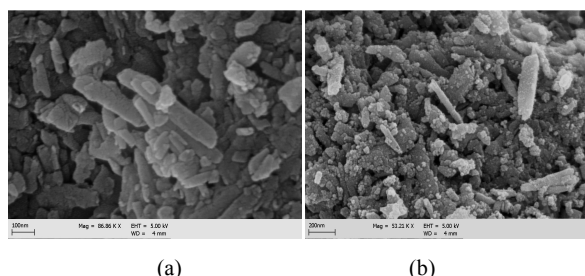

(a)   (b)

Fig. 3 SEM images of: (a) Halloysite powder, (b) HT30 film

The dispersion of halloysite in TiO$_2$ films is obvious but it is firmly agglutinated. No cracks or peeling off traces around halloysite boundaries were observed. The film is permanently attached on the glass substrate with good adherence while halloysite cannot be rived from the composite material. The composite films were finally put at a silver nitrate aqueous solutions in order to silver modify the films. The surface of the films after UV exposure for silver zero valance particles formation on TiO$_2$is presented to the following AFM image of Fig. 4
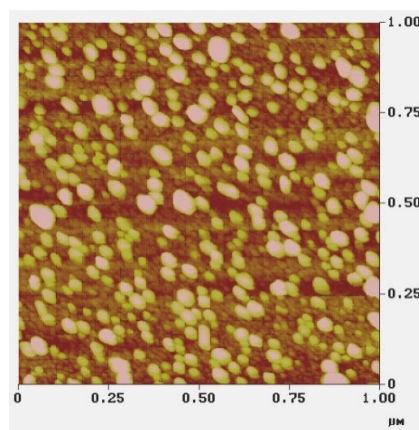

Fig. 4 AFM image of silver modified TiO$_2$ particles

The evidences of SEM images for the nanocomposite material may help us to schematic represent the film fabrication on glass substrates (Fig. 5). It is assumed that the organophilic interphase, assured by X100 surfactant coating, acts like template medium which provides titanium dioxide nanoparticles with relatively monodispersed particle sizes on the surface. The initially amorphous TiO$_2$ phase was crystallized after calcination at 450°C for 15 min in air while X100 was completely burned out.
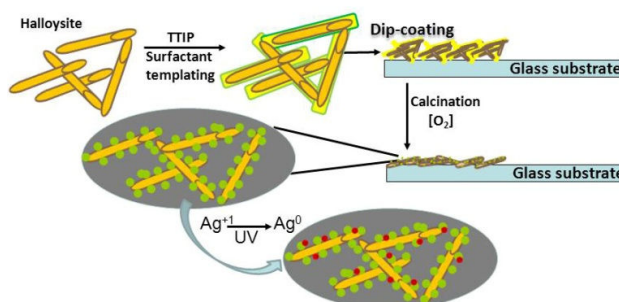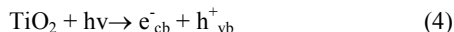

Fig. 5 Preparation procedure for HAL-TiO$_2$ nanocomposite photocatalyst formation as films

Silanol groups (Si-OH) of clay mineral can react with titanium alkoxide giving covalently bonded organic-inorganic derivatives which could be useful for anchoring metal oxide nanoparticles on halloysite surface.

B. Photocatalytic Properties of HAL-TiO$_2$ Composite Films

Titanium dioxide mediated photo-degradation involves the generation of electron-hole pairs [5], which migrate to the photocatalyst surface forming surface bound hydroxyl and superoxide radicals according to the following equations:

$$TiO_2 + hv \rightarrow e^-_{cb} + h^+_{vb} \qquad (4)$$

$$O_2 + e^-_{cb} \rightarrow O_2^{-\bullet} \qquad (5)$$

$$H_2O + h^+_{vb} \rightarrow {}^\bullet OH + H^+ \qquad (6)$$

It is also well known that the hydroxyl and superoxide radicals are the primary oxidizing species in the photocatalytic process. These oxidative reactions result in the photo-discoloration of dyes as target pollutants in water.
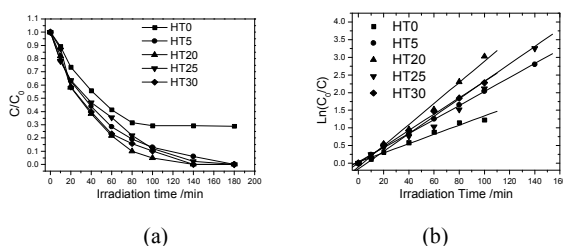

(a)   (b)

Fig. 6 (a) Photo-discoloration of BB-41 for different halloysite - TiO$_2$proportions under UV light,(b) Ln(C$_0$/C) as a function of irradiation time for HAL-TiO$_2$ photocatalysts

Photocatalytic experiments were undertaken on Basic Blue 41 to evaluate HAL-TiO$_2$ composite catalyst in films as shown in Fig. 6. The different weight percentages of halloysite in TiO$_2$ nanocrystalline films showed variations to the photocatalytic activities of the films. The rate of discolorization was monitored with respect to the change in intensity with time of the absorption peak at 610 nm. The absorption peak of the dye diminished with time and disappeared during the reaction indicating that it had been decomposed. Besides, the UV illumination was started after one hour of the photocatalyst presence in dye's sol in order to be in equilibrium before illumination. The results also show that there was no direct photolysis of BB-41 in the absence of any photocatalyst. In the case of HT20 a complete discolorization was reached within 140 min of illumination implied the synergistic effect between clay mineral and TiO$_2$ by preparing highly porous HAL-TiO$_2$ catalysts (Fig. 6 (a)). Moreover, considering the small amount of TiO$_2$ catalyst immobilized onto the substrate, the HAL-TiO$_2$ films were highly efficient to degrade the azo dye. As a consequence, the tubular nanocomposite materials can be an alternative substrate for the growth of nanoparticle TiO$_2$ achieving an efficient photocatalyst. Decomposition kinetics of BB-41 has been observed to follow first-order kinetics and it is well established that photo-discoloration experiments follow Langmuir-Hinshelwood model, where the reaction rate, r, is proportional to the surface coverage, θ, according to the following equation [23]:

$$r = -\frac{dC}{dt} = k_1\vartheta = \frac{k_1 KC}{1+KC} \qquad (7)$$

where k$_1$ is the reaction rate constant, K is the adsorption coefficient of the reactant and C is the reactant concentration. In the case that C is very small, KC factor is negligible in respect to unity and the (7) describes first-order kinetics. The integration of (7) yields to the (8):

$$-\ln(\frac{C}{C_0}) = k_{app}t \qquad (8)$$

With limit condition that on t=0 we have the initial concentration C$_0$. k$_{app}$ is the apparent first-order rate constant. Discoloration kinetics of BB-41 in presence of different HAL proportions in TiO$_2$ nanocrystalline films is presented in Fig. 6b. The maximum value for rate constant was calculated for sample HT20 (29.8x10^{-3} min^{-1}) while the value for pure TiO$_2$ film was estimated at 12.9x10^{-3} min^{-1} (Table II).

TABLE II
CONSTANT OF BB-41 DEGRADATION RATE IN THE PRESENCE OF HALLOYSITE-TIO$_2$ COMPOSITE FILMS MODIFIED WITH SILVER PARTICLES

Sample	k_{app} (x10^{-3} min^{-1}) with no silver	k_{app} (x10^{-3} min^{-1}) with silver
HT0	12.9	18.5
HT5	19.8	19.8
HT20	29.8	26.6
HT25	24.8	25.3
HT30	23.2	28.5

Furthermore, all the samples HAL-TiO$_2$ exhibited better performance than pure TiO$_2$. We mainly attribute this behavior to the internal light scattering because of the presence of the halloysite.

This is also could be attributed to better structural characteristics of the films compared to pure TiO$_2$ film mainly tabulated at porosity and total pore volume. However, the rate of dye discolorization depends on adsorption of the dye into the catalyst porous structure. Finally, it has been found that the same photocatalysts can be used in several photocatalytic cycles without remarkable loss to their efficiency.

C. Photocatalytic Properties of Silver Modified HAL-TiO$_2$ Films

As an alternative procedure to further increase the efficiency of the HAL-TiO$_2$ photocatalysts silver ions were deposited on the TiO$_2$ surface by submerging TiO$_2$ films in aqueous solutions of metal salt for several minutes. It generally believed that silver modified TiO$_2$ could cause a better separation of charge carriers on the oxide surface [24]. Metal cations could be adsorbed onto TiO$_2$ films at substantial quantities because of the relatively high specific surface area of the films. In the case of silver ions and after their adsorption only one electron is enough to reduce silver ions and create zero valence noble metal on the surface of TiO$_2$, according to the following equation:

$$Ag^{+1} + e^- \rightarrow Ag^0 \qquad (9)$$

This electron is easy to be generated, either by UV illumination under black light irradiation or by thermal heating of the films [24].

Indeed, the films after UV exposure were turned to light brownish colored attributed to the creation of zero valence silver due to plasmon resonance absorption [25].
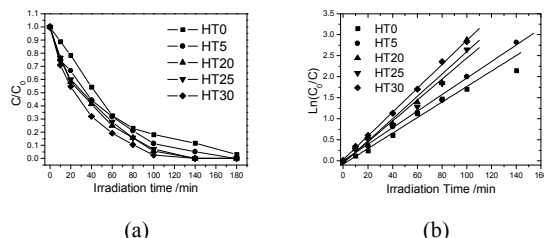

Fig. 7 (a) Photo-discoloration of BB-41 under silver particles modified TiO$_2$ films in presence of different weight percentages of halloysite irradiated with UV light,(b) Ln(C$_0$/C) as a function of irradiation time for silver modified HAL-TiO$_2$ photocatalytic films

The corresponding photocatalytic experiments to evaluate the silver modified HAL-TiO$_2$ composite catalyst in films are shown in Fig. 7 (a). However, the original salt concentration obviously affects the quantity of deposited metal, affected photo-discoloration efficiency. When the silver salt concentration was 10^{-3} mol L^{-1} we obtained the highest photocatalytic efficiency.

At higher metal load, efficiency dropped, possibly due to screening effects. Decomposition kinetics of BB-41 in presence of silver modified HAL-TiO$_2$ films, have been observed to follow first-order kinetics as in the case of bare HAL-TiO$_2$ films. The data are presented in Table II and Fig. 7 (b).
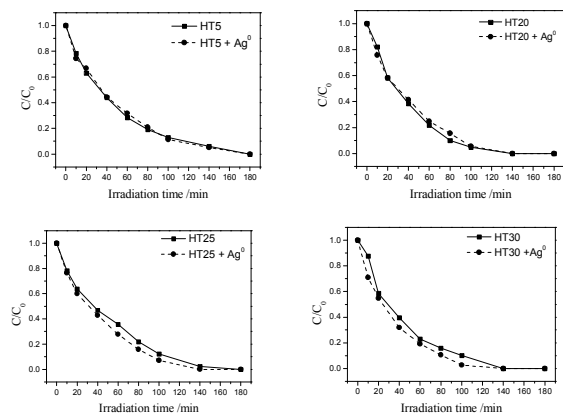

Fig. 8 Comparison between bare and silver modified HAL-TiO$_2$ films to the photo-discoloration of BB-41

In the case of silver modification the most efficient films are proved to be HT30 where a complete discoloration of the dye was achieved within 100 minutes.

For a direct comparison among HAL-TiO$_2$ films and silver modified ones to the photocatalytic decomposition of BB-41, we present the data of Fig. 8.

It is obvious that silver modified films exhibit a slight better performance to the discoloration of BB-41 mainly due to the better separation of charge carriers on the oxide surface. Further experiments with several noble metals modified composite HAL-TiO$_2$ films are under way.

IV. CONCLUSIONS

Nanostructured Halloysite-TiO$_2$ films were synthesized via sol-gel method composed of ethanol, acetic acid, titanium tetraisopropoxide, halloysite nanotubes and nonionic surfactant molecules as organic template. Slow hydrolysis reaction and stable incorporation of inorganic network onto surfactant molecules made it possible to control the subsequent porous nanostructure. The HAL-TiO$_2$ films exhibited enhanced structural properties including crystallinity and active anatase phase while enhanced photocatalytic properties to the discoloration of BB-41 in water were succeeded. The experiments on photocatalytic discoloration of BB-41 implied the importance of synergistic effect between clay mineral nanotubes and TiO$_2$ nanoparticles. In addition, the presence of silver particles on the surface of the composite photocatalyst could further increase the efficiency of the catalyst due to better separation of charge carriers on the TiO$_2$.

REFERENCES

[1] G. A. Umbuzeiro, H.S. Freeman, S. H. Warren, D. P. Oliveira, Y. Terao, T. Watanabe and D. D. Claxton, "The contribution of azo dyes to the mutagenic activity of the Cristais River,"*Chemosp.*, vol. 60, pp. 55-64, June 2005.
[2] Y.E. Benkli, M.F. Can, M. Turan and M.S. Çelik, "Modification of organo-zeolite surface for the removal of reactive azo dyes in fixed-bed reactors," *Water Res.,* vol.39, pp. 487-493, January–February 2005.
[3] E. Forgacs, T. Cserháti and G. Oros, "Removal of synthetic dyes from wastewaters: a review," *Environ.Int.,* vol. 30, pp. 953-971, September 2004.
[4] V. K. Gupta, J. Rajeev, N. Arunima, A. Shilpi and M. Shrivastava, "Removal of the hazardous dye—Tartrazine by photodegradation on titanium dioxide surface,"*Mat. Sci. Engineer.C*, vol. 31, pp. 1062-1067, 2011.
[5] M. I. Litter, "Heterogeneous photocatalysis: Transition metal ions in photocatalytic systems," *Appl. Catal. B: Environ.*, vol. 23, pp. 89-114, November 1999.
[6] X. M. Song, J. M. Wu, and M. Yan, "Photocatalytic degradation of selected dyes by titania thin films with various nanostructures," *Thin Sol. Film.*, vol. 517, pp. 4341-4347, June 2009.

[7] H. Choi, E. Stathatos and D. D. Dionysiou, "Photocatalytic TiO₂ films and membranes for the development of efficient wastewater treatment and reuse systems," *Desalin., vol.* 202, pp. 199-206, January 2007.

[8] H. Choi, E. Stathatos and D. D. Dionysiou, "Synthesis of nanocrystalline photocatalytic TiO₂ thin films and particles using sol–gel method modified with nonionic surfactants," *T. Sol. Films*, vol. 510, pp. 107-114, July 2006.

[9] M. Bizarro, M.A. Tapia-Rodríguez, M.L. Ojeda, J.C. Alonso and A. Ortiz, "Photocatalytic activity enhancement of TiO₂ films by micro and nano-structured surface modification,"*Appl. Surf. Scien., vol.* 255, pp. 6274-6278, April 2009.

[10] V. A. Sakkas, Md. A. Islam, C. Stalikas and T. A. Albanis, "Photocatalytic degradation using design of experiments: A review and example of the Congo red degradation," *J. Haz. Mat.*, vol. 175, 33-44, March 2010.

[11] F. Li, S. Sun, Y. Jiang, M. Xia, M. Sun and B. Xue, "Photodegradation of an azo dye using immobilized nanoparticles of TiO₂ supported by natural porous mineral," J. *Haz. Mat.*, vol. 152, pp. 1037-1044, April 2008.

[12] X. Wang, Y. Liu, Z. Hu, Y. Chen, W. Liu, and G. Zhao, "Degradation of methyl orange by composite photocatalysts nano-TiO₂ immobilized on activated carbons of different porosities," *J. Haz. Mat.,* vol. 169, pp. 1061–1067, September 2009.

[13] G. Rose, M. Echavia, F. Matzusawa and N. Negishi, "Photocatalytic degradation of organophosphate and phosphonoglycine pesticides using TiO₂ immobilized on silica gel,"*Chemosp.*, vol. 76, pp. 595-600, July 2009.

[14] C.-C. Wang, C-K Lee, M-D Lyu and L-C Juang, "Photocatalytic degradation of C.I. Basic Violet 10 using TiO₂ catalysts supported by Y zeolite: An investigation of the effects of operational parameters," *Dyes and Pigm., vol.* 76, pp. 817-824, 2008.

[15] L. Bouna, B. Rhouta, M. Amjoud, F. Maury, M.-C. Lafont, A. Jada, F. Senocq and L. Daoudi, "Synthesis, characterization and photocatalytic activity of TiO₂ supported natural palygorskite microfibers," *Appl. Clay Sci.*, vol. 52, pp. 301-311, May 2011.

[16] T. An, J. Chen, G. Li, X. Ding, G. Sheng, J. Fu, B. Mai and K. E. O'Shea, "Characterization and the photocatalytic activity of TiO₂ immobilized hydrophobic montmorillonite photocatalysts: Degradation of decabromodiphenyl ether (BDE 209)," *Catal. Today*, vol. 139, pp. 69-76, December 2008.

[17] D. Papoulis, S. Komarneni, A. Nikolopoulou, P. Tsolis-Katagas, D. Panagiotaras, H.G. Kacandes, P. Zhang, S. Yin, T. Sato and H. Katsuki, "Palygorskite- and Halloysite-TiO₂ nanocomposites: Synthesis and photocatalytic activity," *Appl. Clay Sci.,* vol. 50, pp. 118-124, September 2010.

[18] D. Papoulis, S. Komarneni, D. Panagiotaras, E. Stathatos, K. C. Christoforidis, M. Fernández-García, H. Li, Y. Shu, T. Sato and H. Katsuki, "Three-phase nanocomposites of two nanoclays and TiO₂: Synthesis, characterization and photacatalytic activities," *Appl. Catal. B: Environ.*, vol. 147, pp. 526-533, April 2014.

[19] E. Stathatos, P. Lianos and C. Tsakiroglou, "Highly efficient nanocrystalline titania films made from organic/inorganic nanocomposite gels," *Micropor. andMesopor. Mat.*, vol. 75, pp. 255-260, November 2004.

[20] E. Stathatos, D. Papoulis, C.A. Aggelopoulos, D. Panagiotarasand A. Nikolopoulou, "TiO₂/palygorskite composite nanocrystalline films prepared by surfactant templating route: Synergistic effect to the photocatalytic degradation of an azo-dye in water," *J. Haz. Mat.,* vol. 211–212, pp. 68-76, April 2012.

[21] E. Stathatos and P. Lianos, F. Del Monte and D. Levy and D. Tsiourvas, "Formation of TiO₂ nanoparticles in reverse micelles and their deposition as thin films on glass substrates,"*Langm.,* vol. 13, pp. 4295-4300, August 1997.

[22] J.–C. Liu, "Mₓ-Oᵧ-Siᵤ Bonding Models for Silica-Supported Ziegler-Natta Catalysts," *Appl. Organometal. Chem.*, vol. 13, pp. 295–302, April 1999.

[23] A.O. Ibhadon, G.M. Greenway, Y. Yue, P. Falaras and D. Tsoukleris, "The photocatalytic activity and kinetics of the degradation of an anionic azo-dye in a UV irradiated porous titania foam," *Appl. Catal. B: Environ.,* vol. 84, pp. 351-355, December 2008.

[24] E. Stathatos, P. Lianos, P. Falaras and A. Siokou, "Photocatalytically Deposited Silver Nanoparticles on Mesoporous TiO₂ Films,"*Langmuir,* vol. 16, pp. 2398-2400, January 2000.

[25] D. Gong, W. Chye, J. Ho, Y. Tang, Q. Tay, Y. Lai, J. G. Highfield and Z. Chen, "Silver decorated titanate/titania nanostructures for efficient solar driven photocatalysis,"*J. Sol. St. Chem.,*vol. 189, pp. 117-122, May 2012.

Dionisios Panagiotaras is holding a BSc in Chemistry from the University of Ioannina Greece (1994) and a Ph.D. in Geochemistry from the University of Patras Greece (2008). He is an Adjunct Assistant Professor in Environmental Geochemistry and Technology at the Department of Mechanical Engineering, Technological Educational Institute (T.E.I.) of Western Greece, Patras, Greece.Dr. Dionisios Panagiotaras research has been published in peer reviewed scientific journals and international conferences. His research interest focused in the field of Low Temperature/Environmental Geochemistry. Specific research interests are clay mineralogy, soil and sediment geochemistry, water chemistry and water-rock interactions, chemical weathering, and environmental uses of nano scale geomaterials such as modified clay minerals-TiO₂ nanocomposites for the decomposition of organic and inorganic pollutants by photocatalytic degradation.

Dimitrios Papoulis is holding a Ph.D. in clay Mineralogy from the University of Patras Greece (2003). He is an Assistant Professor in Mineral recourses emphasizing in clays and clay minerals at the Geology Department of University of Patras, Greece. Dr. Dimitrios Papoulis research has been published in peer reviewed scientific journals and international conferences. His research interest focused in the field of clay mineralogy. Specific research interests are clay minerals genesis, natural recourses, sanitary landfills, clay based nanocomposites: synthesis, characterization and photocatalytic activities in decomposing organic and inorganic pollutants.

Professor Elias Stathatos was born in 1968 in Patras, Greece. He obtained his first degree in Physics from University of Patras and then his Ph.D. degree from Engineering Science Department also in University of Patras. Prof. Stathatos was a postdoctoral research fellow in University of Cincinnati, USA at the Civil&Environmental Engineering Dept. Professor Stathatos is the head of the Nanotechnology and advanced materials laboratory and he has more than 85 publications in peer review journals and four chapters in books which are recognized of more than 2500 citations (*h*-factor=26). He is an editorial board member for Journal of Advanced Oxidation Technologies. His research interests are focused in semiconductors synthesis and characterization. In particular, prof. Stathatos is interested in the conversion of solar into electrical energy using dye-sensitized solar cells employing nanosctuctured materials and also to the heterogeneous photocatalysis based on nanocomposite semiconducting oxides.